Propulsion and Power Research 2012;1(1):29–35

http://ppr.buaa.edu.cn/

Propulsion and Power Research

www.sciencedirect.com

ORIGINAL ARTICLE

Ultrasonic fatigue tests at high temperature on an austenitic steel

D. Wagner[a,*], F.J. Cavalieri[a], C. Bathias[a], N. Ranc[b]

[a]*Laboratoire Energétique Mécanique Electromagnétisme, Université Paris Ouest, 92410 Ville D'Avray, France*
[b]*LMSP, Arts et Métiers-ParisTech, 75013 Paris, France*

Received 17 January 2012; accepted 15 October 2012
Available online 20 December 2012

KEYWORDS

Fatigue;
Gigacycle regime;
High temperature;
Austenitic steel;
Finite element method;
Crack initiation mechanism

Abstract The objective of this paper is to study the gigacycle fatigue behavior of an austenitic steel at temperatures of 600 °C and 700 °C under fully reverse loading ($R=-1$). Numerical simulation by finite element method (FEM) was used to design the specimens and to analyze the effects of the variation in the dynamic Young modulus with temperature from measurements of the ultrasonic resonance frequency. Finally, new stress-life curves for this material are presented for a lifetime range from 10^5 to 10^9 cycles at room temperature, 600 °C and 700 °C.

1. Introduction

One of the main catastrophic causes of failure in propulsion engine is fatigue. An operative life beyond 10^8 cycles is required and it is necessary to investigate the fatigue behavior in the gigacycle range to improve the design. Using classical fatigue criteria, a near hyperbolic relationship between stress and fatigue life is assumed; however, new experimental results show that the fatigue fracture can occur beyond 10^7 cycles, and the concept of endurance limit is not correct [1]. Numerous works have shown that the fatigue behavior of different kinds of materials in the gigacycle regime can be obtained effectively by using ultrasonic fatigue testing machines, and that frequency effects are not important in the determination of the lifetime [2–4]. Many studies in this field have been reported at room temperature [5–7], but available database

*Corresponding author.
E-mail address: daniele.wagner@u-paris10.fr (D. Wagner)

Peer review under responsibility of National Laboratory for Aeronautics and Astronautics, China.

Production and hosting by Elsevier

2212-540X © 2012 National Laboratory for Aeronautics and Astronautics. Production and hosting by Elsevier B.V. All rights reserved.
http://dx.doi.org/10.1016/j.jppr.2012.10.008

Nomenclature

ρ	density
E_{static}	static Young modulus
$E_{dynamic}$	dynamic Young modulus
$U(x)$	amplitude of vibration
k	stiffness constant
L	bar length
f_{reso}	resonance frequency
T	temperature
ω	angular frequency
$A(x)$	cross section of the specimen
L_1	resonance length
L_2	cylindrical length
R_2	radius in the cylindrical section of the specimen
R_1	radius in the central section of the specimen
σ_{max}	maximum stress
A_0	imposed displacement

information at high temperature is very scarce, because the time to reach 10^9 cycles at high temperature using traditional low cycle fatigue testing machines is an almost impossible task to perform. Under these conditions, ultrasonic fatigue testing is a new attractive technique which allows to get fatigue results in a shorter time and with lower costs compared to traditional fatigue procedures.

In this work, we present a methodology to get mechanical and fatigue properties of an austenitic steel subjected to very high cycle loadings ($R=-1$) at high temperatures using the ultrasonic fatigue testing machine and numerical simulations.

2. Material

The material analyzed in this research is an austenitic steel because of its high strength, small Young modulus variation at high temperatures and good resistance to oxidation. The chemical composition is shown in Table 1 and the mechanical properties in Table 2.

Figure 1 shows a general view of the microstructure, where it is possible to see an austenitic structure. Two types of inclusions are presented: very fine intergranular iron and chromium carbides and more massive inclusions rich in Mn, Mo, Nb.

Since Young modulus and density are the dominant variables in ultrasonic tests, it is very important to know their values as accurately as possible. Numerical values at room temperature of the density ρ, static Young modulus E_{static}, and thermal conductivity k are shown in Table 2 as well as the thermal expansion α at 500 °C. The dynamic Young modulus at different temperatures was determined following the procedure presented in Section 5.

Table 1 Chemical composition of the analyzed steel.

Steel	C	Si	Mn	Cr	Ni	W	Nb	N
H854	0.53	0.25	9.5	21	3.8	1	2.2	0.5

Table 2 Thermo mechanical properties of the analyzed steel.

Steel	ρ	E_{static} /(N/mm^2)	UTS /(N/mm^2)	k /(W/(m · K))	α /K^{-1}
H854	7.7	215×10^3	950–1150	14.5	18.8×10^{-6}

3. Experimental procedure

The first ultrasonic fatigue testing machine was introduced by Mason [8]. In the last two decades, research advances in this area have been very important. There are several designs of ultrasonic machines, but they always have three main components [9] (Figure 2):

1) An electric power generator which converts 50 or 60 Hz voltage into ultrasonic 20 kHz electrical sinusoidal signal.
2) A piezoelectric transducer which transforms the electrical signal into mechanical vibration of the same frequency.
3) An ultrasonic horn that amplifies the vibration coming from the transducer in order to obtain the required stress amplitude in the middle section of the specimen.

The generator is connected to a PC using an A/D acquisition card for controlling the generator and the piezoelectric actuator that induced the mechanical movement. The transducer generates a mechanical wave

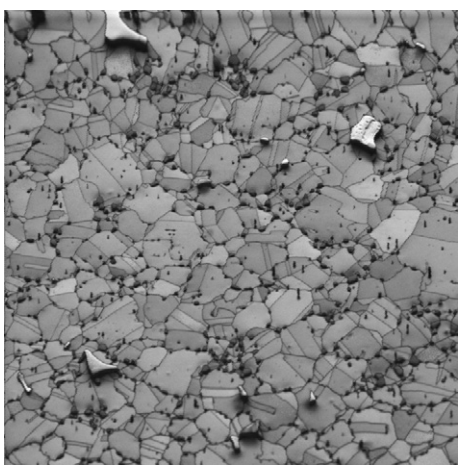

Figure 1 Austenitic microstructure of the analyzed material.

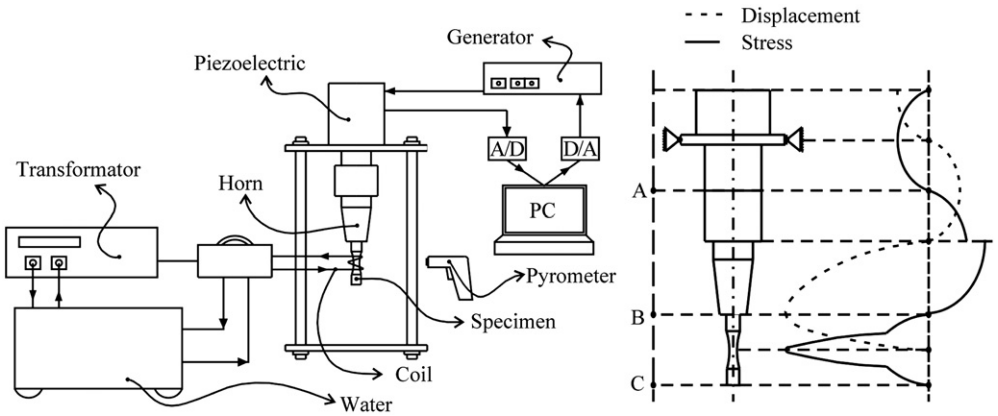

Figure 2 Fatigue testing machine and vibratory stress and displacement field.

with an intrinsic frequency of 20 kHz and for this reason, the specimen must be designed with this same natural frequency in its first mode of vibration. In this way, the specimen reaches a maximum displacement (null stress) at the end and maximum stress (null displacement) in the central section, see Figure 2.

This type of machine is used for fatigue life analysis at more than 10^5 cycles. The operative frequency range goes from 19.5 to 20.5 kHz, and if it decreases below 19.5 kHz or increases above 20.5 kHz, the test is stopped automatically. In contrast with the low and mega cycle fatigue tests, where the machine has a natural frequency different from the specimen, in the ultrasonic fatigue machines the specimen-machine forms a resonance system in which the displacement amplitudes are kept constant during the test at a pre-selected value. In the tests, the machine stops automatically when a crack propagates rapidly causing a change in the resonance frequency of the system.

The mechanical system works in the elastic regime, and consequently the relationships between displacement, strain and stress are linear. In the machine used in this work, the electrical voltage is also linear and proportional to the displacement. The ultrasonic fatigue testing machine calibration is required to make the system vibrate in resonance at an ultrasonic frequency of about 20 kHz. The calibration was performed with a cylindrical specimen and a laser displacement sensor situated at one specimen end, which registers displacements from 1 μm to 199.9 μm with a resolution of 0.1 μm.

In the room temperature tests, the central part of the specimen is cooled with fresh air.

An induction coil technique was used in the tests at high temperatures. The coil was made of a spirally shaped copper tube situated in the middle of the specimen, in order to heat the specimen around its middle section at a given temperature. An optical pyrometer was used during the tests to measure and control the temperature at the center of the specimen. Its emissivity was calibrated with a reference instrument. Thermocouples have also been used to calibrate the pyrometer and to measure the temperature during the tests. The pyrometer presents some practical advantages compared to thermocouples, because it does not require any welding to the specimen allowing measurements at different points in a very easy way.

4. Analytical and numerical models for designing a specimen

In dynamic loading, by taking a bar and neglecting the transversal contraction, the natural frequency is given by:

$$f_{\text{reso}} = \frac{1}{2L}\sqrt{\frac{E_{\text{d}}}{\rho}} \tag{1}$$

where E_{d} is the dynamic Young modulus which considers the dynamic effects and it is usually different from the static Young modulus, ρ the density and L the bar length.

4.1. Experimental procedure for dynamic Young modulus determination

So, the knowledge of the dynamic modulus E_{d} is essential and the relationship between E_{d} and temperature, $E_{\text{d}}=E_{\text{d}}(T)$ is therefore required for designing a specimen in an ultrasonic load regime at high temperature. We have determined the dynamic Young modulus at the resonant frequency of a cylindrical specimen, first at room temperature and later at high temperature, using the gigacycle fatigue testing machine and numerical simulations by FEM.

In order to determine E_{d} at room temperature, a cylindrical specimen initially of length $L=(2f_{\text{reso}})^{-1}(E_{\text{static}}/\rho)^{0.5}$ (see Eq. (1)) was designed with the static Young modulus (Table 2) and a resonance frequency $f_{\text{reso}}=20$ kHz. Since tests displayed a natural frequency lower than 20 kHz, the specimen was cut until obtaining experimentally $f_{\text{reso}}=20$ kHz. The final dimension of the cylindrical bar was 132.1 mm. Finally, the dynamic Young modulus was obtained as $E_{\text{d}}=\rho(2L20.000)^2$.

Table 3 Temperature and frequency values measured on cylindrical specimen (unit: °C).

Cases	I	II	III	IV	V	VI	VII
L_1=15 mm	20	53	100	96	130	150	210
L_2=32 mm	20	76	152	200	240	330	420
L_3=64 mm	20	100	200	300	400	500	550
L_4=94 mm	20	80	155	250	340	430	500
L_5=113 mm	20	65	130	200	300	380	400
Freq./kHz	19.98	19.89	19.82	19.73	19.64	19.54	19.50
FEM/kHz	20.00	19.89	19.819	19.734	19.65	19.52	19.52
Error/%	0.1	0	0.005	0.02	0.05	0.1	0.12

An induction coil was used for heating a cylindrical specimen. Temperature was measured with an optical pyrometer as well as with thermocouples connected along the length of the specimen. Seven tests were conducted, registering the temperatures in different points of the specimen together with its resonance frequency, as shown in Table 3. Here, L_i is the length from the top of the specimen to the measured point. The maximum temperature is located at point L_3. Measurements of resonance frequency were performed in the gigacycle fatigue testing machine for a cylindrical specimen at seven different temperature conditions (cases from I to VII). By adjusting coefficients of a quadratic function, the dynamic Young modulus variation in terms of temperature was finally approximated as:

$$E_{\mathrm{d}}(T) = 2.01134 \times 10^{11} - 1.09468 \times 10^{7} T - 7417.87 T^{2} \quad [\mathrm{Pa}] \tag{2}$$

where T is given in °C (see Figure 3).

When using this expression in the modal analysis, the computed vibration frequencies approximated the experimental values with an error less 0.12% as shown in Table 3.

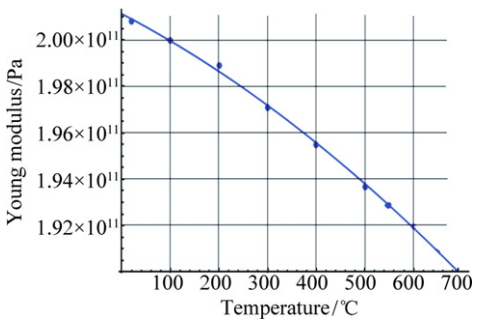

Figure 3 Dynamic Young modulus vs. temperature for the analyzed steel.

4.2 Specimen design

In a typical ultrasonic fatigue specimen the length of the cylindrical part of the specimen is adjust to ensure the resonance of the system.

Then, the resonance length L_1 can be shown to be:

$$L_1 = \frac{1}{k}\tan^{-1}\left\{\frac{1}{k}[\beta\coth(\beta L_2) - \alpha\tanh(\alpha L_2)]\right\} \tag{3}$$

where

$$\beta = \sqrt{\alpha^2 - k^2} \tag{4}$$

$$\alpha = \frac{1}{L_2}\cosh^{-1}\left(R_2/R_1\right) \tag{5}$$

$$k = \omega\sqrt{\frac{\rho}{E_{\mathrm{d}}}} \tag{6}$$

For the material used in this work (see Tables 1 and 2 together with Eqs. (3–6)) L_1 at 20 kHz becomes 23.75 mm.

A modal analysis with an axisymmetric FEM model was also performed in order to make a comparison. The resonance frequency in the FEM model using the geometry obtained with the analytical equations was 20.0188 kHz. The resonance length was modified until obtaining a resonance frequency of 20 kHz. The final dimension of L_1 proposed by FEM was 23.8 mm. We used the geometry obtained by FEM calculation for the tests; nevertheless, we should mention that the solution of both methods is in good agreement. The dimensions of the specimen used for room temperature tests are shown in Figure 5.

Experimental results obtained on the gigacycle testing machine showed that the designed specimen vibrated with a natural frequency of 19.985 kHz.

Afterwards, the stress and displacement fields were computed using both FEM mechanical analysis and the analytical equations.

When a specimen is heated, the resonance frequency is affected by geometric changes and by the decrease of the Young modulus produced by the thermal effects. Consequently, the specimen geometry has to be modified in order to keep a natural frequency of vibration at the desired temperature as close as possible to 20 kHz. In other words, the resonance length of the specimens used at high temperature should be shorter than that used for room temperature [10,11].

The temperature distribution on the specimen was determined experimentally using a pyrometer and thermocouples on a specimen whose dimensions were not the definitive ones for the tests at high temperatures.

Particularly, to carry out this task, we used a room temperature specimen. The experimentally measured temperatures on the specimen were registered at the points A, B, C, D and E as it is shown in Figure 4 for the temperature cases of 600 °C and 700 °C.

Finally, by fitting the data, the temperature as a function of the position can be approximated by:

$$T_{600}(x) = 217.062 + 18701.8x - 231487x^2 \quad [^\circ\mathrm{C}] \qquad (7)$$

$$T_{700}(x) = 234.739 + 23053.5x - 289105x^2 \quad [^\circ\mathrm{C}] \qquad (8)$$

where x is given in mm. By using Eqs. (7) and (8) and the Young modulus as a function of temperature $E_d = E_d(T)$ (Eq. (2)), the dynamic Young modulus variation along the length of the specimen, $E_d = E_d[T(x)]$, was established for different temperature cases. The final resonance length for the desired temperature was obtained.

Final dimensions of the specimens for the temperature cases of 600 °C and 700 °C are shown in Figure 5.

5. Experimental results and discussions

Firstly, room temperature fatigue tests were performed. Then, the tests at temperatures of 600 °C and 700 °C were carried out. Specimens which did not fail up to 10^9 cycles were considered runouts, and incremental stress was applied to them until obtaining the fatigue rupture. Specimens were polished to reduce the scatter as much as possible in the S–N curve.

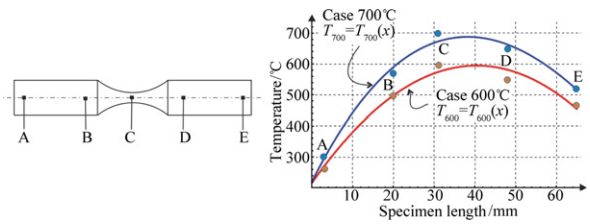

Figure 4 Temperature measured points on non-cylindrical specimen.

Temperature/℃	Resonance length/mm
20	L_1=23.8
600	L_1=20.00
700	L_1=20.00

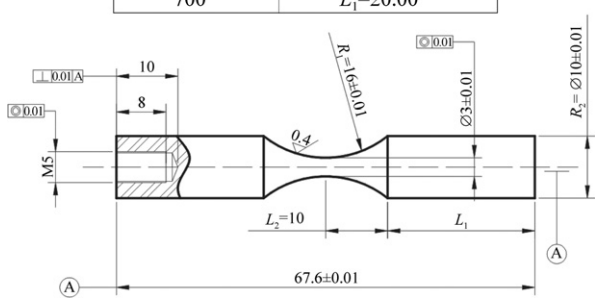

Figure 5 Ultrasonic fatigue specimen geometry for different temperatures.

The stress life response of the material tested at room temperature (RT) is shown in Figure 6 in a semi-logarithm plot, in Figures 7 and 8 for 600 °C and 700 °C. The behavior at RT is specific. The highest cycles number for a failed specimen was 2×10^7 cycles. The scattering is more important than at 600 °C or 700 °C. At RT, the endurance limit is about 353 MPa, whereas at 600 °C or 700 °C, the S–N curve decreases until 10^9 cycles. Often, in gigacycle fatigue, the crack is initiated from an internal defect, inclusion, or pore. For this material, in all tests, except one at 600 °C, the cracks were initiated at a surface location and no interior crack initiations from inclusions were found. In the only "fish eye" found, the crack initiation was due to a massive inclusion rich in Nb, whose diameter is about 40 μm (Figure 9). For the all other specimens, the crack initiation was caused by the effect of stress

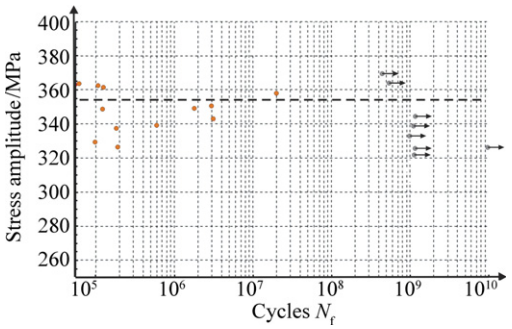

Figure 6 S–N curve at room temperature for the material analyzed.

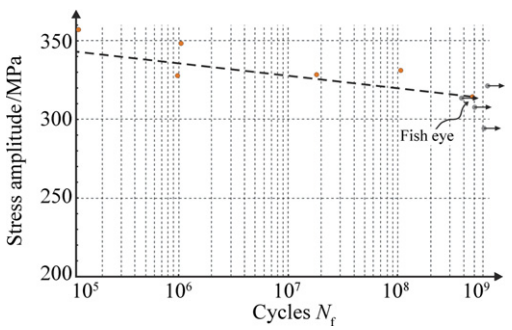

Figure 7 S–N curve at 600 °C for the material analyzed.

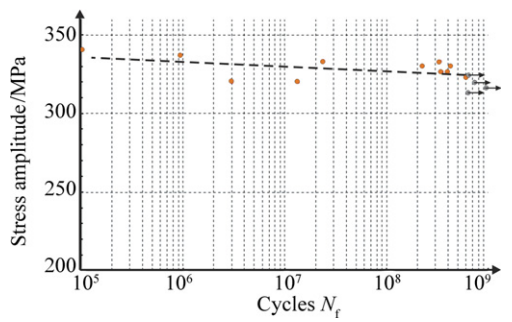

Figure 8 S–N curve at 700 °C for the material analyzed.

heterogeneity and stress concentration related to persistent slip bands (PSB) formation.

This austenitic steel is face centered cubic structure with a low stacking fault energy. In this case, the cross lip is not favoured and the twinning occurs leading to the delay of PSB formation [12]. A sample test at RT which runs out up to 10^9 cycles without failing was cut in the central part. A polished section has been observed in SEM (Figure 10) where we can see mechanical twins.

Electron Back Scattering Diffraction (EBSD) observations were performed on a polished section (perpendicular to the longitudinal axis) taken in the central part of the specimen or taken at the end of the specimen. For the 2 locations, we did not observe phase transformation: the microstructure remains austenitic. But, on the other hand, the volume fraction of twinning has increased between the 2 locations. It is 0.18 on the polished section at the specimen end and 0.25 in the central part specimen (Figure 11 which is the EBSB observation of Figure 1).

It seems, when the sample has not failed at 10^9 cycles, the PSB formation is delayed due to the twinning deformation. So, at RT, the deformation mode is either twinning (no PSB formation and not failure) or gliding (with PSB formation and failure).

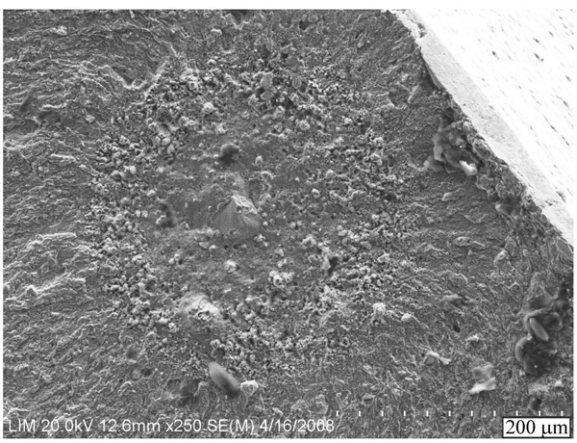

Figure 9 Zoom amplification at inclusion.

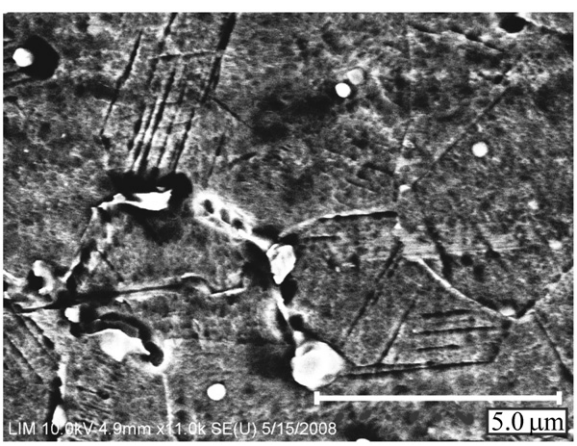

Figure 10 SEM image on a specimen not failed at 10^9 cycles.

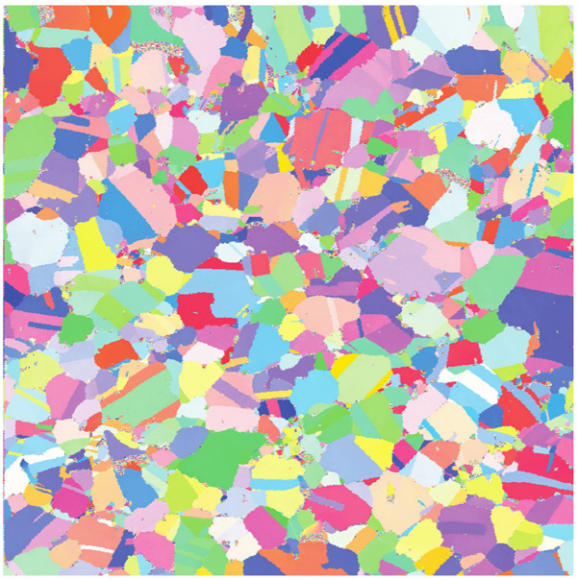

Figure 11 EBSB observation of a polished section in the central part of the specimen (not failed at 10^9 cycles).

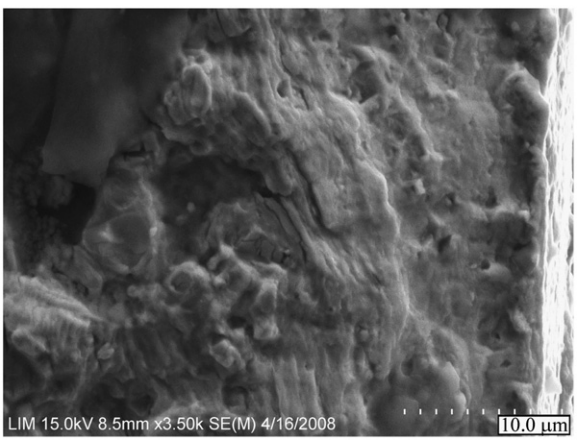

Figure 12 SEM image on a failed specimen at RT (a twin is visible at the bottom on the left).

At high temperature, the stacking fault energy has increased, and the cross lip is always possible with formation of PSB. SEM observations of fracture surface at RT show mechanical twins (Figure 12), whereas at high temperature, no twins are visible.

6. Conclusions

The ultrasonic fatigue technique was developed to determine fatigue behavior of austenitic steels in a range of 10^6 to 10^9 cycles under fully reverse loading at high and room temperature. The most important conclusions obtained are summarized below:

1) The dynamic mechanical properties of austenitic steel subjected to high temperatures were identified

based on numerical simulations and the measured resonance frequency of the specimens.

2) The design of specimens for high temperature tests using FEM modal analysis, showed good agreement with the experimental tests. When the specimen reached the desired temperature, i.e., room temperature, 600 °C or 700 °C, resonance frequency was close to 20 kHz during the ultrasonic fatigue test.
3) At room temperature, more than 20 specimens were tested and none failed above 2×10^7 cycles. For the non failed specimens, a deformation by twinning (delaying PSB formation) seems to be present.
4) The 600 °C and 700 °C *S–N* curve have shown a continuous decreasing stress-life response.
5) In the specimens tested, the crack initiation was observed on the surface (except for one specimen).

References

[1] C. Bathias, L. Drouillac, P. Le Francois, How and why the fatigue S–N curve does not approach a horizontal asymptote, International Journal of Fatigue 23 (1) (2001) 143–151.
[2] C. Bathias, P.C. Paris, Gigacycle Fatigue in Mechanical Practice, Marcel Dekker, New York, 2005.
[3] H. Mayer, Fatigue crack growth and threshold measurements at very high frequencies, International Materials Reviews 44 (1) (1999) 1–34.
[4] L.E. Willertz, Ultrasonic fatigue, International Materials Reviews 25 (1) (1980) 65–78.
[5] I. Marines, G. Dominguez, G. Baudry, J.-F. Vittori, S. Rathery, J.-P. Doucet, C. Bathias, Ultrasonic fatigue tests on bearing steel AISI-SAE 52100 at frequency of 20 and 30 kHz, International Journal of Fatigue 25 (9) (2003) 1037–1046.
[6] E. Bayraktar, I.M. Garcias, C. Bathias, Failure mechanisms of automotive metallic alloys in very high cycle fatigue range, International Journal of Fatigue 28 (11) (2006) 1590–1602.
[7] B. Zettl, H. Mayer, C. Ede, S. Stanzl-Tschegg, Very high cycle fatigue of normalized carbon steels, International Journal of Fatigue 28 (11) (2006) 1583–1589.
[8] W.P. Mason, Piezoelectronic Crystal and Their Application in Ultrasonics, Van Nostrand, New York, 1950, p. 161.
[9] C. Bathias, Piezoelectric fatigue testing machine and devices, International Journal of Fatigue 28 (11) (2006) 1438–1445.
[10] A. Shyam, C.J. Torbet, S.K. Jha, J.M. Larsen, M.J. Caton, C.J. Szczepanski, T.M. Pollock, J.W. Jones, Development of ultrasonic fatigue for rapid, high temperature fatigue studies in turbine engine materials, Superalloys, The Minerals, Metals and Materials Society, Seven Springs, Pennsylvania, USA, 2004, pp. 259–268.
[11] J.Z. Yi, C.J. Torbet, Q. Feng, T.M. Pollock, J.W. Jones, Ultrasonic fatigue of a single crystal Ni-base superalloy at 1000 °C, Materials Science and Engineering 443 (1) (2007) 142–149.
[12] C. Bathias, A. Pineau, Fatigue des matériaux et des structures 1, Lavoisier, Paris, 2008.